Hindawi Publishing Corporation
Journal of Electrical and Computer Engineering
Volume 2013, Article ID 627410, 5 pages
http://dx.doi.org/10.1155/2013/627410

Research Article

Radar Array Diagnosis from Undersampled Data Using a Compressed Sensing/Sparse Recovery Technique

S. Costanzo,[1] A. Borgia,[1] G. Di Massa,[1] D. Pinchera,[2] and M. D. Migliore[2]

[1] *DIMES, Università della Calabria, 87036 Rende, Italy*
[2] *DIEI, Università di Cassino e del Lazio Meridionale, Via Di Biasio 43, 03043 Cassino, Italy*

Correspondence should be addressed to S. Costanzo; costanzo@deis.unical.it

Received 24 May 2013; Accepted 20 August 2013

Academic Editor: Alvaro Rocha

A Compressed Sensing/Sparse Recovery approach is adopted in this paper for the accurate diagnosis of fault array elements from undersampled data. Experimental validations on a slotted waveguide test array are discussed to demonstrate the effectiveness of the proposed procedure in the failures retrieval from a small set of measurements with respect to the number of radiating elements. Due to the sparsity feature of the proposed formulation, the method is particularly appealing for the diagnostics of large arrays, typically adopted for radar applications.

1. Introduction

The identification of failures in array antennas is an important problem that have addressed large attention both in academies and industries. It is well known that the presence of fault elements in arrays causes a performance degradation in terms of both gain and sidelobe levels. This is particulary important in case of high performance arrays with very low sidelobes, largely adopted in radar applications.

The back-propagation algorithm [1] is the most widely adopted approach to detect fault array elements. It is based on the Fourier relationship between the fields on the array aperture and the measurement plane, with a number of samples satisfying the Nyquist theorem. However, using the standard half-wavelength sampling step, the number of measurement points and consequently the time required for data acquisition turns out to be very large.

Broadly speaking, it is possible to obtain a data reduction by introducing tighter a priori information on the source. For example, in the last couple of decades, an effective theory to reduce the set of data in antenna measurements under a priori knowledge of the antenna shape [2] has been successfully applied to near-field measurements [3, 4]. Using different a priori information, for example, on the spatial correlation of the sources, a further decrease in the number of measurements can be achieved [5]. Efficient algorithms have been also introduced in the literature to obtain accurate antenna far-field characterization from near-field measurements performed on strategic scanning surfaces with reduced acquisition points [6–8].

The approach proposed in [9], and based on the matrix inversion method, can be also adopted to obtain a reduction of data by introducing a proper model of the source. However, it generally requires a set of measurements not smaller than the number of array elements.

Recently, Compressed Sensing/Sparse Recovery (CS/SR) techniques [10, 11] have been proposed in antenna diagnosis, first from near-field data [12] and more recently from far-field measurements [13]. The application of CS/SR techniques potentially allows a number of data that increases linearly with the number of failures but only logarithmically with the number of radiating elements, thus allowing a large reduction in the amount of measured data as well as in the acquisition time.

In this paper, an experimental validation of the CS approach proposed in [12] for a proper detection of fault array elements is provided for the first time. For illustrative purpose, a small linear array well known in the literature, namely, a slotted waveguide array, is assumed as a test structure. Near-field measurements on a reduced number of points

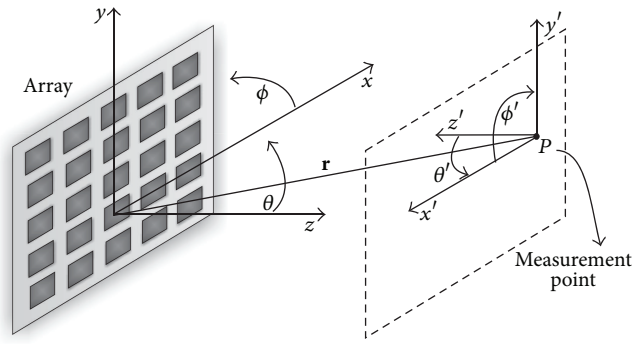

Figure 1: Problem geometry.

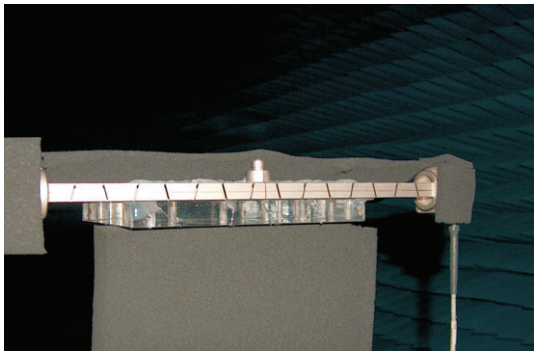

Figure 2: Photograph of slotted waveguide array (AUT) into anechoic chamber at the University of Calabria.

with respect to the number of array elements are successfully adopted to accurately identify the failures positions, thus demonstrating the effectiveness of the proposed CS approach on undersampled data.

2. Outline of the Method

Let us consider (Figure 1) an array under test (AUT) consisting of N radiating elements located at known positions $\mathbf{r}_n$. Let x_n and $\mathbf{f}_n(\theta, \phi)$ be the excitation coefficient and the electric-field radiation pattern of the nth radiating element, respectively. A probe having effective height $\mathbf{h}(\theta, \phi)$ is placed into M spatial points $\mathbf{r}_m$, $m = 1, \ldots, M$. The voltage at the probe output can be expressed by a linear system of the kind:

$$\mathbf{Ax} = \mathbf{y}, \tag{1}$$

wherein $\mathbf{y} = (\mathbf{y}_1, \mathbf{y}_2, \ldots, \mathbf{y}_n)^{\mathbf{T}} \in \mathbf{C}^{\mathbf{M}}$, y_m is the probe voltage measured at point $\mathbf{r}_m$, $\mathbf{x} = (\mathbf{x}_1, \ldots, \mathbf{x}_N)^{\mathbf{T}} \in \mathbf{C}^{\mathbf{N}}$, $\mathbf{A} \in \mathbf{C}^{\mathbf{M}\times\mathbf{N}}$ is a matrix whose (m, n) element is equal to $\exp(-j\beta r_{m,n})/(4\pi r_{m,n})\mathbf{f}(\theta_{m,n}, \phi_{m,n}) \cdot \mathbf{h}(\theta'_{m,n}, \phi'_{m,n})$, $r_{m,n} = |\mathbf{r}_m - \mathbf{r}_n|$, and $\theta_{m,n}$ and $\phi_{m,n}$ are the relative angles between the mth measurement point and the nth element position in a reference system centered on the nth array radiating element.

In the present work, the problem of identification of fault elements into array antennas is considered. If assuming a number S of failures, this goal can be achieved by inverting

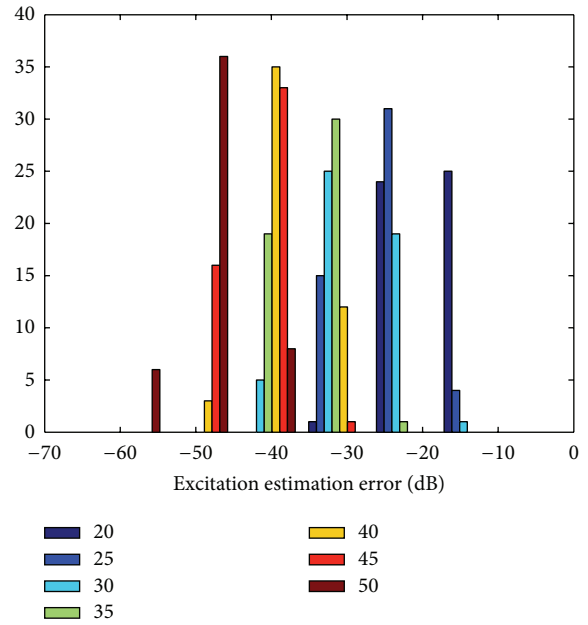

Figure 3: Histogram (simulations) of MSE of the ℓ_1 solution: $S = 2$, $M = 11$, and SNR ranging from 20 dB up to 50 dB.

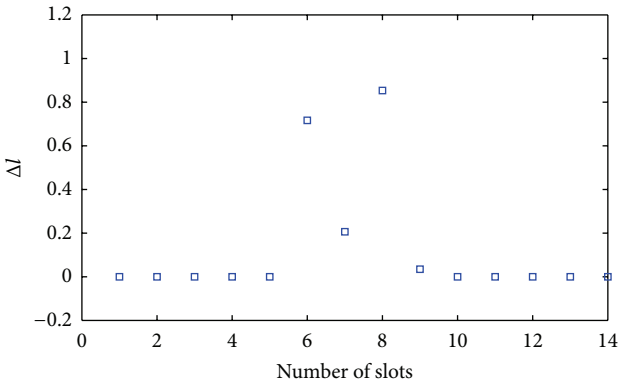

Figure 4: The difference between exact and estimated excitations (simulations) with failures at positions $n = 6$ and $n = 8$: $S = 2$, $M = 11$, and MSE = 20 dB.

the system (1), as proposed in [9], but requiring that $M \geq N$. Let us suppose $S \ll N$, as usually happens.

As first step, we suppose to know (by measurements or available model/simulation) the field radiated by the failure-free array into M measurement points, thus obtaining a reference data vector $\mathbf{y}^r$. The relative excitations of the reference (failure-free) array are denoted by vector $\mathbf{x}^r$. In a successive step, we collect the field radiated by the array with fault elements, thus obtaining a second vector $\mathbf{y}^d$ with associated excitations $\mathbf{x}^d$. Now, let us consider the linear system (1), with

$$\begin{aligned} \mathbf{x} &= \mathbf{x}^r - \mathbf{x}^d, \\ \mathbf{y} &= \mathbf{y}^r - \mathbf{y}^d; \end{aligned} \tag{2}$$

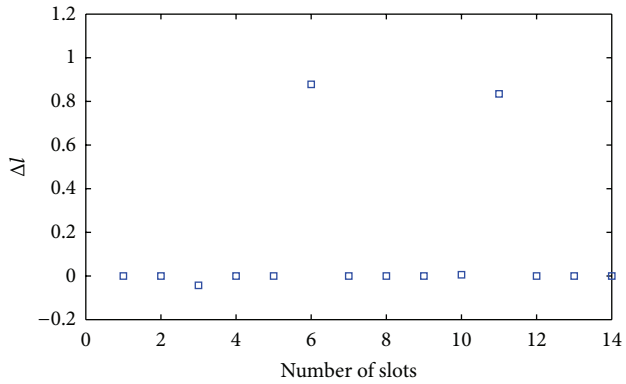

FIGURE 5: The difference between exact and estimated excitations (simulations) with failures at positions $n = 6$ and $n = 11$: $S = 2$, $M = 11$, and MSE = 25 dB.

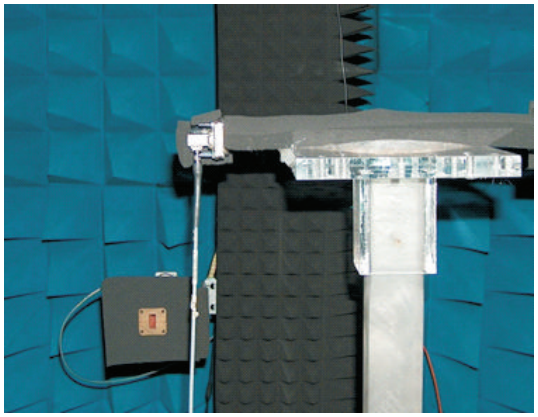

FIGURE 6: Photograph of measuring probe into anechoic chamber at the University of Calabria.

x and **y** are named as "innovation" vectors. Since $S \ll N$, we have an equivalent problem involving a highly sparse array.

Accordingly, the problem is *sparse*; that is, the unknown vector has only a small number of not null entries, and it can be solved by the following constraint minimization:

$$\begin{aligned} &\min_{\mathbf{x}} \quad \|\mathbf{x}\|_1 \\ &\text{subject to} \quad \|\mathbf{A}\mathbf{x} - \mathbf{y}\|_2 \leq \epsilon, \end{aligned} \tag{3}$$

wherein ϵ is related to the noise affecting the data.

3. Numerical Results

As a preliminary step, extensive numerical simulations are performed to check the performance of the failure detection algorithm, by assuming a slotted-waveguide array well characterized in the literature to be AUT [14], with $N = 14$ radiating elements (Figure 2). The slotted array is terminated into a matched load, thus working as a nonresonant array and producing a main lobe tilted with respect to the broadside direction [15].

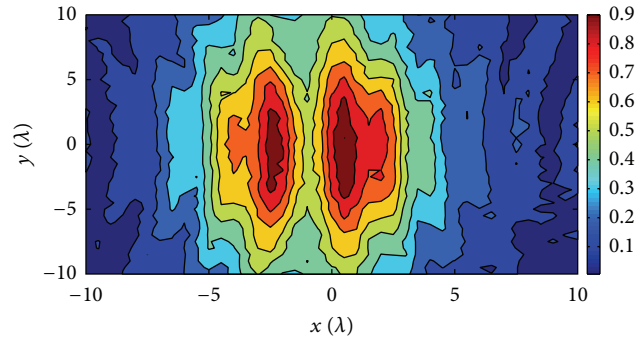

FIGURE 7: Measured near-field amplitude on the failure-free slotted waveguide array.

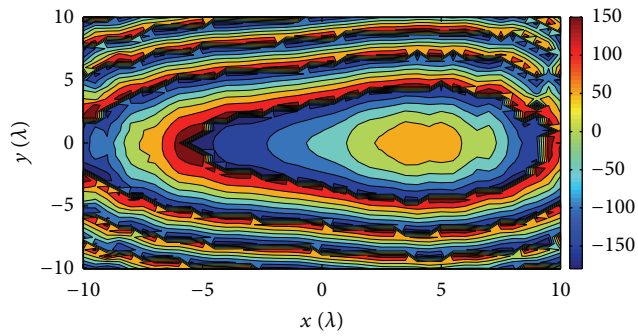

FIGURE 8: Measured near-field phase on the failure-free slotted waveguide array.

To check the robustness of the CS technique, various simulations are initially performed by considering different numbers of failures and data affected by Gaussian noise. As an example, the histogram of the Mean Square Error (MSE) in the reconstruction of the array excitations is reported in Figure 3, by considering 50 trials in the presence of $S = 2$ failures randomly chosen among the $N = 14$ elements and assuming $M = 11$ measurements affected by a Signal-to-Noise Ratio (SNR) ranging from 20 dB up to 50 dB.

In order to have a qualitative information on the value of MSE required to accurately identify the failures, an example of faults reconstruction is reported in Figures 4 and 5 by assuming a MSE equal to 20 dB and 25 dB, respectively. The plots indicate that a value of MSE equal to 20 dB is not sufficient for an accurate failures identification, while a value of 25 dB gives good results. Accordingly, results depicted in Figure 3 indicate that $M = 11$ measurements assure an accurate detection of failures with high probability in the case of SNR greater than 30 db. Such a noise level is easily reached in near-field measurements.

4. Setup Description and Experimental Results

In order to validate the CS approach for fault-arrays diagnosis, a planar near-field setup is assumed by adopting a slotted-waveguide array (Figure 2) as AUT and a standard X-band rectangular waveguide (Figure 6) as measuring probe.

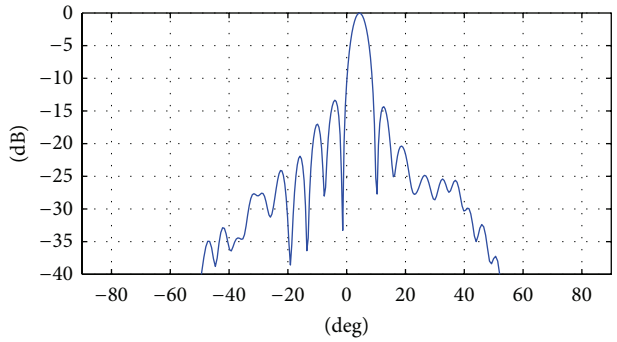

Figure 9: Far-field pattern of failure-free slotted waveguide array (result from planar near-field to far-field transformation).

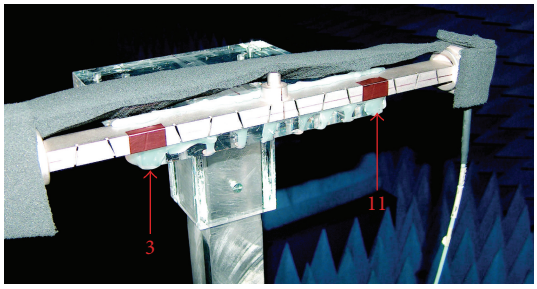

Figure 10: Photograph of slotted waveguide array with failures at positions $n = 3$ and $n = 11$.

The proper operation of the test array is first verified by performing near-field measurements on a planar grid of 41×41 $\lambda/2$ spaced points and then applying the standard planar near-field to far-field transformation. An operating frequency $f = 10$ GHz is chosen. The contour plots of near-field amplitude and phase on the measurement plane placed 40 cm away from the AUT are reported in Figures 7 and 8, respectively. The corresponding far-field pattern along the array plane, illustrated in Figure 9, shows a main lobe properly pointing at an angle approximately equals 5°, as imposed by the array theory [15].

To apply the proposed CS technique, a second set of near-field data is collected on the slotted array by assuming the presence of two failures (namely, with the 3rd and 11th slots covered by a conductive material), as illustrated in Figure 10. The measured near-field amplitudes on the failure-free and two-fault arrays are reported in Figure 11 along the central line of the acquisition domain.

To perform the experimental validation, only a subset of near-field data illustrated in Figure 11 is adopted. In particular, $M = 11$ points are assumed, which are equivalent to a field undersampling at a 2λ spacing. As outlined in the previous section, the ℓ_1 minimization is applied to the difference of the fields plotted in Figure 11, and the corresponding result of Figure 12, giving the difference between the excitation coefficients of the failure-free and the two-faults array, clearly identifies the failures at positions $n = 3$ and $n = 11$. It is worth stressing that we use only $M = 11$ measurements to estimate $N = 14$ excitations. As a comparison, the result obtained

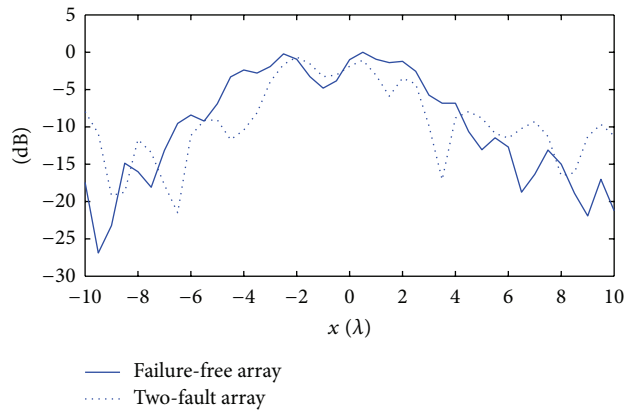

Figure 11: Measured near-field amplitude [dB] in the absence and presence of failures (slots 3 and 11 closed).

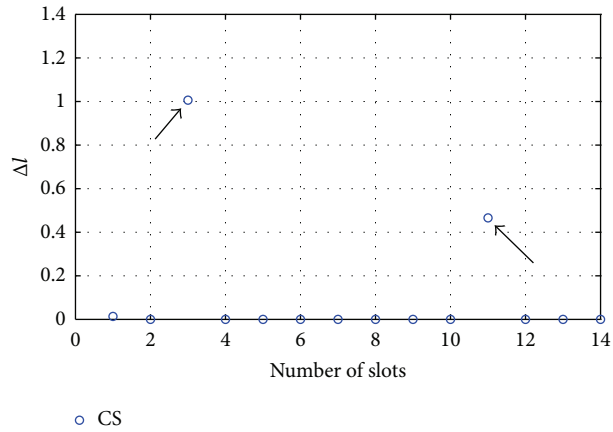

Figure 12: ℓ_1 minization: the difference of excitations in the absence and the presence of failures (slots 3 and 11 closed).

using the linear inversion method by pseudoinverse [16] is plotted in Figure 13, showing a poor identification of the fault elements in this case.

5. Conclusion

The problem of arrays diagnostics has been faced in this work by adopting a Compressed Sensing/Sparse Recovery approach able to give an equivalent sparse formulation of the problem relative to the identification of fault elements.

Due to the sparsity feature, the method is able to detect arrays failures from a set of largely undersampled data compared to the one obtained using standard Nyquist sapling step.

The validity of the approach has been tested on a standard slotted waveguide array, by artificially creating critical configurations, and results have demonstrated an accurate identification of the failure positions using a number of measured data smaller than the number of the radiating elements of the array.

In the experimental example, the reduction of the measurements compared to the standard $\lambda/2$ sampling step

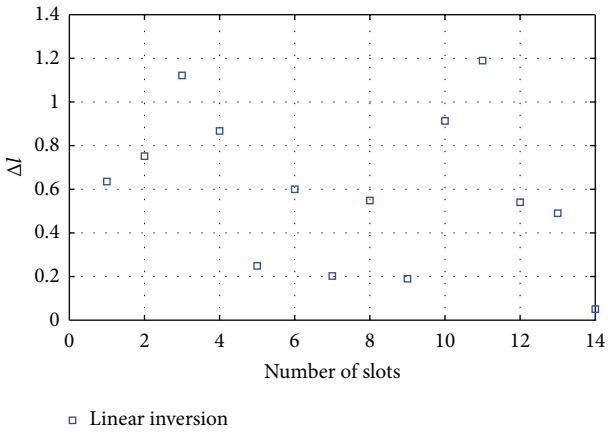

FIGURE 13: ℓ_2 minization: the difference of excitations in the absence and the presence of failures (slots 3 and 11 closed).

adopted in near-field measurements is relatively modest, that is, 4 times. However, it is worth recalling that, broadly speaking, the number of measurements required by the proposed technique mainly depends on the number of failures, while other techniques not based on Sparse Recovery require a number of measurements that depend on the electrical dimensions of the antenna under test. Consequently, the small dimensions of the array here adopted for the experimental validations do not make so clear the advantages of the technique when testing high-performance radar antennas with thousands of elements distributed on 2D surfaces, for which a much more significant reduction in the number of measurements is expected [12].

References

[1] J. J. Lee, E. M. Ferren, D. P. Woollen, and K. M. Lee, "Near-field probe used as a diagnostic tool to locate defective elements in an array antenna," *IEEE Transactions on Antennas and Propagation*, vol. 36, no. 6, pp. 884–889, 1988.

[2] O. M. Bucci, C. Gennarelli, and C. Savarese, "Representation of electromagnetic fields over arbitrary surfaces by a finite and non redundant number of samples," *IEEE Transactions on Antennas and Propagation*, vol. 46, pp. 361–369, 1998.

[3] O. M. Bucci and M. D. Migliore, "A new method for avoiding the truncation error in near-field antennas measurements," *IEEE Transactions on Antennas and Propagation*, vol. 54, no. 10, pp. 2940–2952, 2006.

[4] S. Costanzo, G. Di Massa, and M. D. Migliore, "A novel hybrid approach for far-field characterization from near-field amplitude-only measurements on arbitrary scanning surfaces," *IEEE Transactions on Antennas and Propagation*, vol. 53, no. 6, pp. 1866–1874, 2005.

[5] M. D. Migliore, "An informational theoretic approach to the microwave tomography," in *Proceedings of the IEEE International Symposium on Antennas and Propagation and USNC/URSI National Radio Science Meeting (APSURSI '08)*, San Diego, Calif, USA, July 2008.

[6] S. Costanzo and G. Di Massa, "Far-field reconstruction from phaseless near-field data on a cylindrical helix," *Journal of Electromagnetic Waves and Applications*, vol. 18, no. 8, pp. 1057–1071, 2004.

[7] S. Costanzo and G. Di Massa, "Direct far-field computation from bi-polar near-field samples," *Journal of Electromagnetic Waves and Applications*, vol. 20, no. 9, pp. 1137–1148, 2006.

[8] S. Costanzo and G. Di Massa, "Near-field to far-field transformation with planar spiral scanning," *Progress in Electromagnetics Research*, vol. 73, pp. 49–59, 2007.

[9] O. M. Bucci, M. D. Migliore, G. Panariello, and P. Sgambato, "Accurate diagnosis of conformal arrays from near-field data using the matrix method," *IEEE Transactions on Antennas and Propagation*, vol. 53, no. 3, pp. 1114–1120, 2005.

[10] E. J. Candes and T. Tao, "Near-optimal signal recovery from random projections: universal encoding strategies?" *IEEE Transactions on Information Theory*, vol. 52, no. 12, pp. 5406–5425, 2006.

[11] D. L. Donoho, "Compressed sensing," *IEEE Transactions on Information Theory*, vol. 52, no. 4, pp. 1289–1306, 2006.

[12] M. D. Migliore, "A compressed sensing approach for array diagnosis from a small set of near-field measurements," *IEEE Transactions on Antennas and Propagation*, vol. 59, no. 6, pp. 2127–2133, 2011.

[13] G. Oliveri, P. Rocca, and A. Massa, "Reliable diagnosis of large linear arrays: a bayesian compressive sensing approach," *IEEE Transactions on Antennas and Propagation*, vol. 60, no. 10, pp. 4627–4636, 2012.

[14] S. Silver, *Microwave Antenna Theory and Design*, McGraw-Hill, New York, NY, USA, 1949.

[15] R. E. Collin, *Antennas and Radiowave Propagation*, McGraw-Hill, New York, NY, USA, 1987.

[16] G. Golub and C. F. Van Loan, *Matrix Computation*, John Hopkins University Press, Baltimore, Md, USA.